

**2017 NDIA GROUND VEHICLE SYSTEMS ENGINEERING AND TECHNOLOGY  
SYMPOSIUM  
MODELING & SIMULATION, TESTING AND VALIDATION (MSTV) TECHNICAL SESSION  
AUGUST 8-10, 2017 - NOVI, MICHIGAN**

**PHYSICAL TESTING AND MODELING OF BOLTED AND WELDED  
CONNECTIONS FOR ARMORED VEHICLE MODELS**

**Michalis Hadjioannou, PhD  
Matt Barsotti  
Eric Sammarco, PhD, PE  
David Stevens, PhD, PE**  
Protection Engineering Consultants LLC  
Austin, TX

**ABSTRACT**

*Protection Engineering Consultants (PEC) has performed static and dynamic-pendulum tests on bolted and welded connection sub-assemblies to generate data for development and validation of modeling approaches capable of accurately predicting the behavior of connections exposed to shock loads. The connections consisted of Rolled Homogeneous Armor (RHA) steel plates, Grade 8 bolts, and fillet welds of ER80-S wire, as typically used in armored vehicles. A summary of the forty physical tests on nine connection configurations are provided along with strain gage and Digital Image Correlation (DIC) data. The specimens were designed to have typical failure modes, i.e. bolt shear, plate tear-out, and weld shear fracture. Using these data, high-fidelity numerical models were developed, with exceptionally good comparisons to the experimental data. During the development of the numerical models, crucial modeling parameters were identified and were shown to have significant influence to the calculated response.*

**INTRODUCTION**

As part of the United States Marine Corps (USMC) Mitigation of Blast Injuries through Modeling and Simulation project, Protection Engineering Consultants (PEC) performed static and dynamic physical tests of bolted and welded connections under high load rates. The tests were designed to populate experimental data for the development of accurate yet efficient numerical modeling techniques for connections that are exposed to shock loads. Such loading conditions result from blast, landmine detonation, ballistic impact and vehicle collisions. Accurate representation of the connection behavior in large vehicle models is important and metrics such as energy absorption, ductility, and fracture of a connection have crucial impact on vehicle model response and casualty predictions.

The physical tests were performed for connections loaded in direct shear using Rolled Homogeneous Armor (RHA) steel plates, Grade 8 bolts, and fillet welds of ER80-S 0.035 wire with 75-25 gas mix. Static tests were performed with a universal testing machine and dynamic tests were performed with a 2,250 lb pendulum that impacted a specially designed frame that loaded the connection specimens in direct shear. A total of forty static and

dynamic tests were performed in two rounds on nine different bolted and welded connection configurations. Initial tests were used to check the overall loading procedure, acquire and correlate strain gage data and Digital Image Correlation (DIC) data, and ensure that the specially designed loading frame used in the dynamic tests was able to sustain the severe dynamic loading. In the main tests, the specimens were designed to have different failure modes, i.e. bolt shear, plate tear-out, and weld shear fracture. Similar specimens were impacted with increasing pendulum velocities to assess the effects associated with high rate loading.

The experimental data from the connection tests were analyzed and post-processed to inform the development of high-fidelity numerical models for simulation of the full connection loading histories for the static and dynamic tests as well as to predict the failure modes. The high-fidelity numerical models were built in LS-DYNA<sup>®</sup>. The intention was to minimize modeling assumptions by having accurate representations of the specimens both in physical geometry and mechanical properties. All of the test components, i.e. steel plates, bolts, washers, nuts, steel members, etc. were finely discretized with solid elements and interacted with

each other through contact definitions. Pretension was also applied to the bolted connection specimens using a non-iterative approach of LS-DYNA.

While the ultimate goal of this effort was to develop reduced modeling techniques that provide accurate results in a reasonable amount of time [1], [2], the work presented in this paper focuses on the development of the high-fidelity numerical models and important findings for accurate representation of the full connection behavior until failure.

## PHYSICAL TESTING

The numerical modeling approaches presented herein were validated against specially designed experimental tests in which bolted and welded connections were tested under dynamic and quasi-static loading. All tests were performed at Southwest Research Institute (SwRI) under subcontract from PEC. The tests applied direct shear loads to bolted and welded connections as shown in Figure 1.

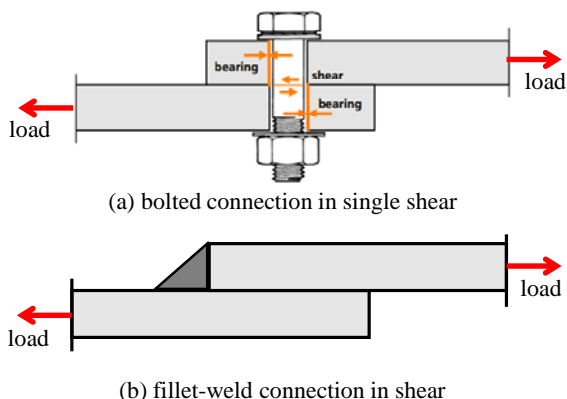


**Figure 1: Connection load in direct shear, (a) bolted, (b) fillet-weld.**

A universal testing machine was used for the static tests, shown in Figure 2(a), with a displacement rate that ranged from 0.05-in/min to 0.10-in/min and was representative of quasi-static loading conditions. Figure 2(b) shows the 2,250 lb pendulum used for the dynamic tests. The pendulum impacted a specially designed frame that applied tensile force to the connection specimen and ultimately loaded the connection in direct shear (Figure 1).

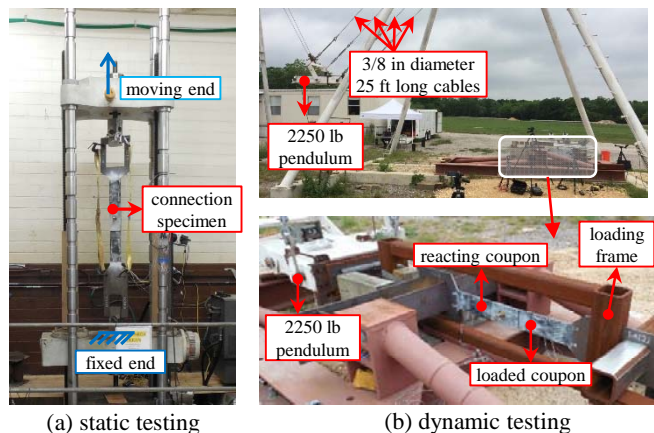


**Figure 2: Testing apparatus used for the experimental tests, (a) static testing, (b) dynamic testing.**

A total of forty static and dynamic tests were performed on nine different configurations of bolted and welded connections in two rounds. The connection configurations included an array of different plate thicknesses (0.25-in, 0.375-in, and 0.75-in), bolt diameters (0.50-in and 0.75 in), bolt-hole to edge distances (0.875-in, 1.125-in, and 3-in on center), bolt pretension levels, and weld lengths (3-in or 6-in long and 0.25-in thick). All specimens were comprised of materials that are typically used in armored vehicles: rolled homogeneous armor (RHA) steel plates; SAE Grade 8 bolts and ER80-S 0.035 welds with 75-25 gas mix. Among the different specimen configurations, typical failure modes were obtained, including plate tear-out failure, bolt shear fracture, and weld fracture. These three failure modes are shown in Figure 3.

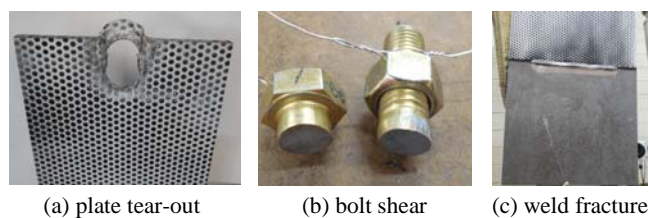


**Figure 3: Typical failure modes of physical tests, (a) plate tear-out, (b) bolt shear, (c) weld fracture.**

The strain histories were measured at discrete locations at the vicinity of the connection using a combination of strain gages and a Digital Image Correlation (DIC) system as depicted in Figure 4. Additionally, in the static tests a load cell recorded the applied tensile force to the specimens. The pendulum impact velocity was measured with an accelerometer that was rigidly attached to the pendulum. The recorded data provided the basis for the development and validation of high-fidelity numerical models that

realistically simulated both the pendulum and quasi-static tests.

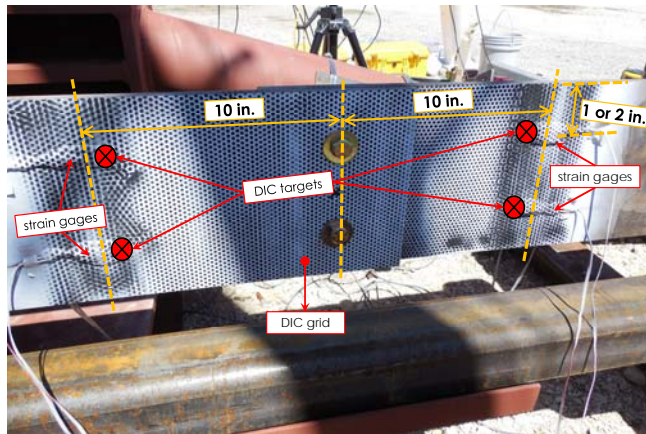


Figure 4: Instrumentation of a connection specimen.

## DETAILED NUMERICAL MODELS

All simulations of the physical tests were performed using the general purpose, multi-physics Finite Element (FE) code LS-DYNA. The exact geometry of the test specimens including the RHA plates, Grade 8 bolts, washers, welds, and crucial components of the testing apparatus were constructed and discretized with three-dimensional Lagrangian brick elements. The objective was to minimize simplifying assumptions on the numerical models and to therefore reduce any sources of error and inaccuracies that usually occur when assumptions are made. Figure 5 shows two views of the FE model of a single bolted connection specimen and the associated FE model of the test apparatus for static and dynamic testing respectively. Interaction between all components was realized through contact definitions.

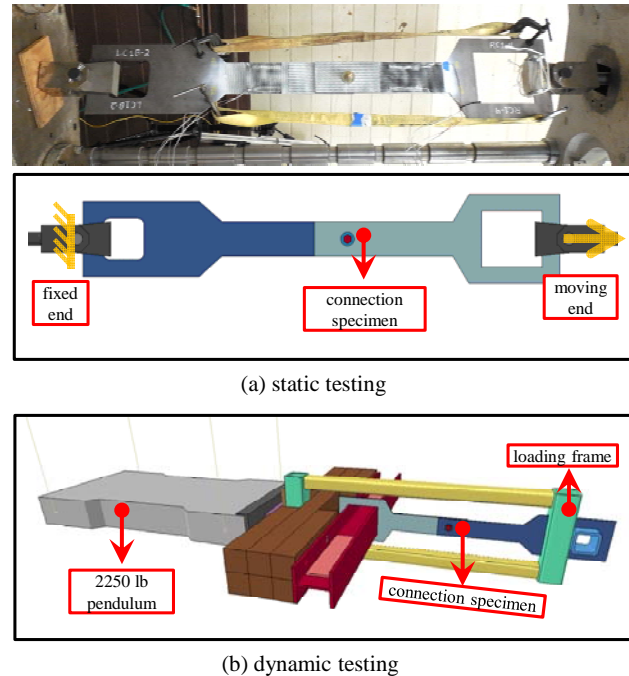


Figure 5: FE models simulating the physical tests, (a) static testing, (b) dynamic testing.

### Meshing

The discretization of the connection specimens was dictated by their dimensions and the size of elements that had to be used for accuracy. Also, parts that interacted through contact definitions were meshed with similar size elements for enhanced accuracy. The thinnest RHA plate had a nominal thickness of 0.25-in and was discretized with three fully-integrated 8-node brick elements over the thickness while maintaining an approximate aspect ratio of 3:1. Regardless of the plate thicknesses, a minimum of three elements was deemed necessary to capture the through-thickness stress gradient. Another important consideration was the discretization of the plate close to the bolt-hole and the closest free edge, particularly in cases that plate tear-out was expected. It was found that at least four elements had to be placed in that region to capture plate tear-out correctly as depicted in Figure 6.

The bolts/washers/welds were predominantly meshed with 8-node brick elements and only a few tetrahedral elements as needed because of geometry restrictions. A total of sixteen elements were used across the diameter of the bolt shank and six elements over the weld edges. Because the bolts/washers interacted through contact definitions with the RHA plates, it was important to avoid dissimilar mesh sizes. Relatively large size differences in the meshes that interact through contact tend to reduce the accuracy of the contact algorithm. Finally, the fillet welds

(Figure 1b) were idealized as triangular prisms and were meshed using similar principles to those used for the plates.

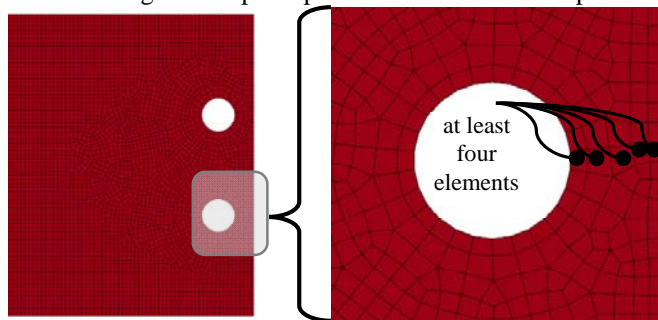


**Figure 6: Mesh close to the free edge of a bolt-hole.**

### **Material Parameters**

The material properties for the specimen components were determined with physical tests. Samples from the RHA coupons and Grade 8 bolts were tested in uniaxial tension at load rates ranging from  $0.01\text{-sec}^{-1}$  to  $100\text{ sec}^{-1}$ . A summary of the obtained values are presented in Table 1. It is noted that weld material was not tested and material properties found in the literature were used.

RHA armor plate		Grade 8 bolts	
Strain Rate ( $\text{sec}^{-1}$ )	Ultimate Stress (ksi)	Strain Rate ( $\text{sec}^{-1}$ )	Ultimate Stress (ksi)
0.01	177	0.01	161
0.1	177	0.1	164
1	179	1	166
10	182	10	169
100	186	33	172

**Table 1: Dynamic mechanical properties of steel components.**

The Johnson-Cook plasticity model [3] was used to represent the RHA steel plates, Grade 8 bolts, and ER80-S weld material. Supplementary experimental data [4], [5] were used to determine the damage parameters of the plasticity model. Those parameters account for the different ductility limits of steel depending on its stress state, which is defined as the triaxiality factor (the ratio of the hydrostatic stress to the Von-Mises stress). The damage parameters were proven to be important in obtaining the correct response of the bolted connections.

For the components of the testing apparatus such as the loading frame, pendulum, specimen clamps (Figure 5), nominal material parameters were sufficient because these components were oversized to remain elastic during testing, which was confirmed during the tests.

### **Contact Definitions**

Interaction between the individual components of the tests was explicitly simulated with contact definitions. Segment-based contact was invoked for the simulations, as it was found to behave better compared to the LS-DYNA default penalty-based contact [6]. The segment-based contact eliminates the possibility of nodes penetrating into the other part while in some cases the penalty-based contact might not. The static and dynamic friction coefficient was specified to 0.5 and 0.4. A 20% contact damping was applied as suggested from LS-DYNA [7] for metals that interact with each other.

### **Bolt Pretension**

The pretension of the bolted specimens was considered in the simulations. A special algorithm was invoked in LS-DYNA [6] to apply a specified stress in the bolts before any other loads are applied. This approach does not require any iterations from the user to achieve the desired pretension load, something that is required when pretension is applied with thermal contraction.

## **COMPARISONS WITH EXPERIMENTAL DATA**

The FE models shown in Figure 5 were used to replicate the physical tests. All specimen configurations were analyzed with LS-DYNA and were validated against the experimental data. Validation of the numerical simulations was based on direct comparisons against the recorded experimental data and the failure modes. Figure 7 shows a summary of the three failure modes (plate tear-out, bolt shear fracture, weld fracture) observed during the physical tests, and failure modes that were numerically obtained from models replicating the same test. Crucial parameters to capture these failure modes correctly are discussed in a subsequent section.

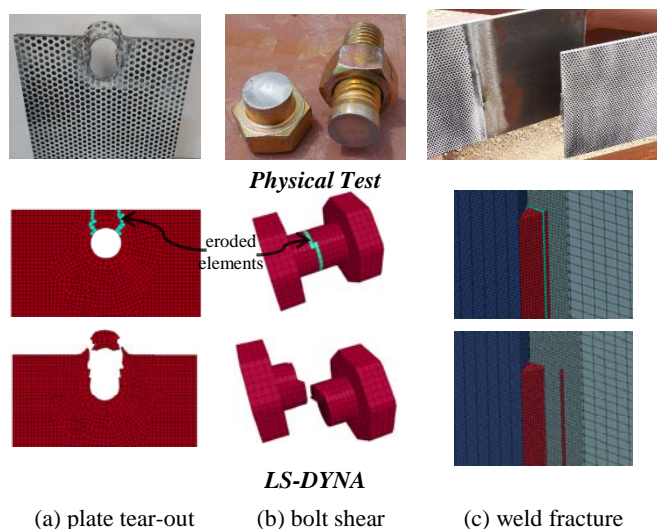


**Figure 7: Failure modes of tests and LS-DYNA simulations, (a) plate tear-out, (b) bolt shear, (c) weld fracture.**

### Pendulum Tests Comparisons

Strain histories from the pendulum tests were compared with strain histories from the numerical models. Strains parallel to the direction of loading were recorded at four discrete locations for each specimen as depicted in Figure 4. Strains histories were exported from the numerical models at the same locations. Figure 8 shows a comparison of the strain histories in a specimen with two 0.75-in diameter bolts, with 0.25-in and 0.375-in thicknesses on the loaded and reacting coupons (Figure 2b) respectively. The impact velocity of the pendulum in this test was 230-in/sec (13-mph) and the loaded plate had tear-out fracture (Figure 7a). In Figure 8, time=0 is approximately the time that the pendulum strikes the loading frame and the specimen is loaded. The duration of the loading is about 5-msec after which the connection fails because of plate tear-out fracture. It can be seen that the LS-DYNA analysis captured with good accuracy both the load duration and the strain history. It is noted that the strains in the loaded coupon tended to be higher from those on the reacting coupon because of the smaller thickness of the former. The fluctuations in the numerically obtained strain histories are attributed to the perfect positioning of the interacting parts. For example because the bolt was perfectly centered to the bolt-hole, this results in relative sliding (equal to the clearance of the bolt and the bolt-hole) between the two plates and eventually a pulse at the time that the bolt shank bears against the two plates. On the other hand, in the physical tests it is likely that some parts were not perfectly centered to their neighboring components which eliminated some of those fluctuations in the strain histories.

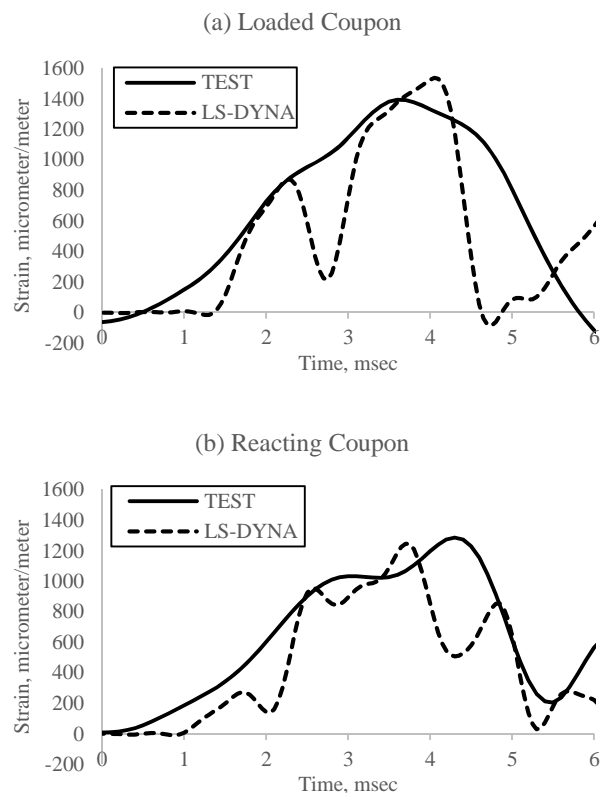


**Figure 8: Strain comparison of a pendulum test with two 0.75-in diameter bolts struck with 230-in/sec, (a) loaded coupon, (b) reacting coupon.**

Another point of comparison is the peak axial force for each physical test, which was calculated using the peak recorded strain. Assuming that the strain was approximately uniform over the entire cross-section and by multiplying the peak strain with the elastic modulus of steel and the cross-sectional area of the plate, an estimate of the peak axial force for each specimen was obtained. From the numerical simulations, the peak axial force was directly calculated by integrating the strain histories at the same location (Figure 4) that the strains were measured in the physical tests. Figure 9 summarizes the peak axial force comparisons between different tests at the different impact velocities. It can be seen that the experimental data compare fairly well with the data from the numerical simulations. It is noted that the data points that are connected with lines correspond to the same specimen configuration that was struck at different pendulum impact velocities.

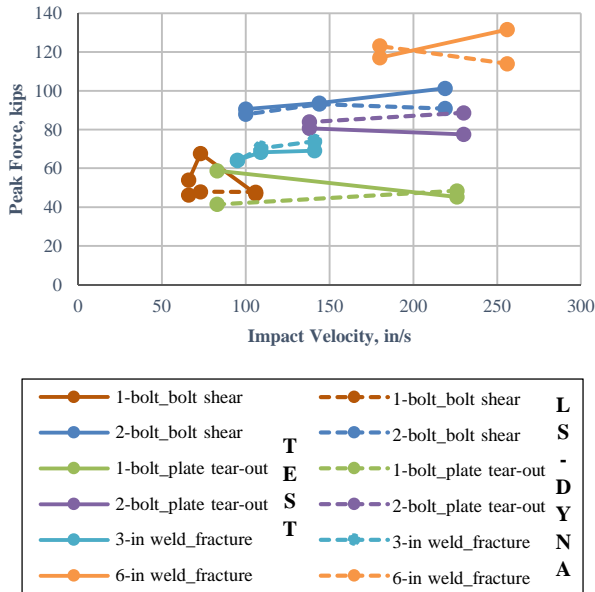


**Figure 9: Peak force versus impact velocity, experimental data and LS-DYNA simulations.**

**Static Test Comparisons**

The load-displacement histories from the static tests compared fairly well with the results obtained from the numerical simulations (Figure 2a). Figure 10 shows the load-displacement response of two specimens that were tested statically. Both specimens had a single 0.75-in diameter bolt. Their only difference was the edge distance of the bolt-hole to the free edge perpendicular to the loaded direction. The distances were 0.875-in and 3-in which resulted in plate tear-out and bolt shear fracture respectively. It can be seen that in both cases the results from LS-DYNA are in good agreement with the experimental data. It is noted that the flat plateau of about 5-kips is the stage that the two plates slide relative to each other until the bolt shank starts to bear against the opposite edges of the bolt holes (Figure 1a). The difference in the length of this plateau is because in the numerical models the bolt is perfectly centered to the bolt holes whereas in the physical specimens this was not practically possible.

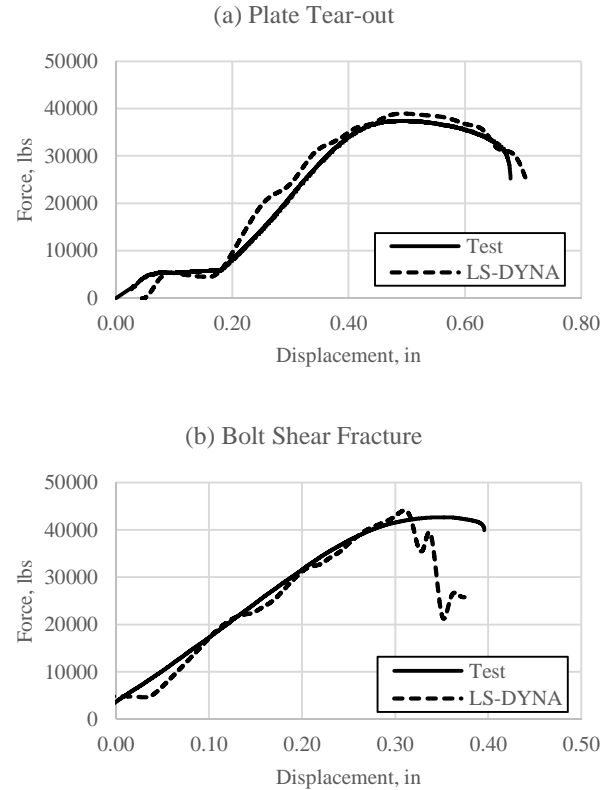


**Figure 10: Load-displacement comparison of the static tests with a single, 0.75-in diameter bolt specimen failing in: (a) plate tear-out and (b) bolt shear fracture.**

**MODELING HIGHLIGHTS**

During the development and validation phase of the numerical models, a number of important parameters were identified as crucial in obtaining accurate and phenomenologically correct response for the specimens. Two of the most crucial parameters are highlighted in the following subsections.

**Triaxiality Failure Criteria**

Correctly modeling steel fracture for the simulations presented herein was essential. A widely accepted but problematic method to simulate fracture of steel is to specify erosion (deletion) criteria. A common deletion criterion is the peak plastic strain at fracture. However, this simple criterion is applied irrespective of the stress state (tension or compression) which causes fictitious elements deletions. Previous tests from a number of different researchers including Johnson and Cook [3] and Whittington *et al.* [4] suggest that steel ductility is a function of its stress-state.

A value that quantifies the stress-state is the triaxiality factor, which is the ratio of the hydrostatic stress to the Von-Mises stress. Certain material laws in LS-DYNA, including the Johnson-Cook material law [3], allow the definition of a triaxiality dependent erosion criterion, which makes a drastic difference in the obtained response, especially when plate tear-out fracture was the anticipated failure mode. The triaxiality failure criterion resulted in a more realistic block shear failure compared to the simple peak plastic strain at fracture. Figure 11 shows a comparison of a bolted connection specimen that was statically loaded until plate tear-out fracture. Although the peak connection capacity is calculated correctly, the ductility and energy dissipation that causes the connection to fracture is considerably under-predicted when triaxiality is not employed. Correct prediction of the connection ductility has implications when connections are analyzed in high-transient simulations such as impact or blast loads.

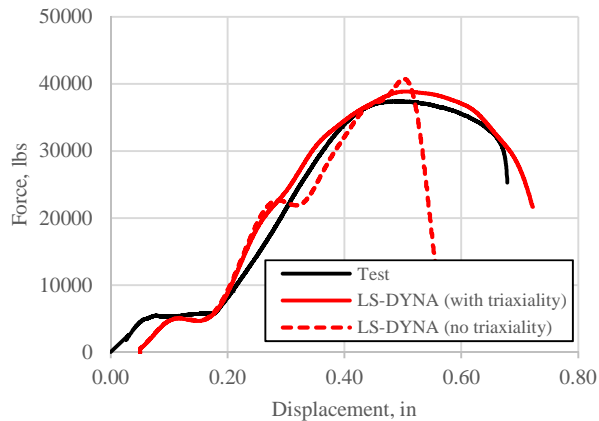


**Figure 11: Load-displacement response of a bolted specimen.**

Figure 12 also shows a comparison of the obtained failure modes. When triaxiality-dependent failure (Figure 12a) is invoked the block shear fracture is more realistic and similar to the experimentally obtained one (Figure 7a). If plastic strain at fracture does not vary with triaxiality (Figure 12b), elements that are highly compressed due to the bearing of the bolt shank against the bolt-hole are fictitiously deleted.

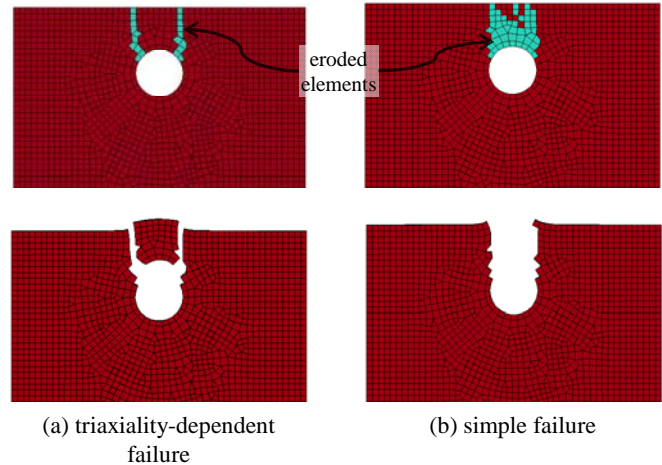


**Figure 12: Bolt tear-out fracture with: (a) triaxiality-dependent failure, (b) triaxiality-independent failure.**

### **Shear Plane and Bolt Shank Nodes**

Another interesting observation during the development of the numerical models was related to the bolt shear fracture. It was found that the bolt shear fracture was more realistic when a plane of nodes of the bolt shank coincided with the shear plane of the bolt (Figure 1a). Figure 13 shows a comparison of the obtained failure modes when nodes of the bolt shank coincided and did not coincide with the shear plane. The physical tests indicate that the fractured plane of the bolts is relatively flat and parallel to the shear plane. However, in cases that nodes of bolt shank were not placed at the shear plane of the bolt (Figure 13b) the fractured plane of the bolt was less flat and not parallel to the shear plane. The remedy for that issue was to ensure that the shear plane and nodes of bolt shank coincide (Figure 13a).

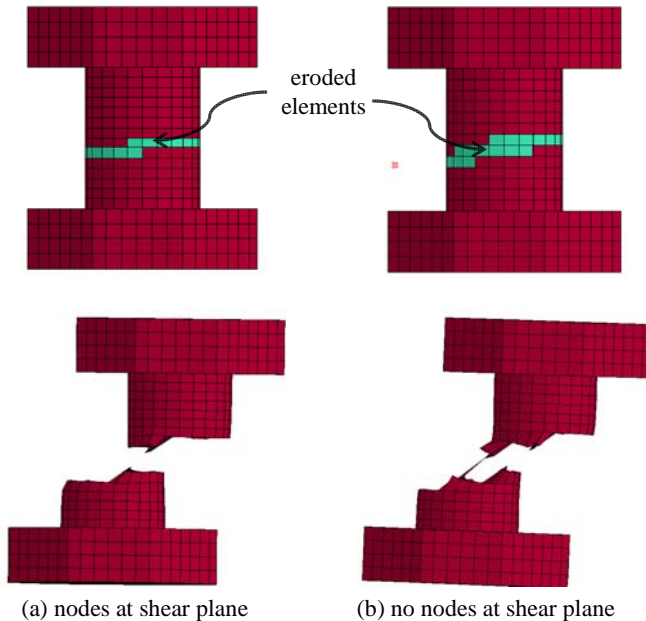


**Figure 13: Bolt shear fracture when the nodes of the bolt shank and shear plane: (a) coincide (b) differ.**

## SUMMARY

A total of forty static and dynamic (pendulum) tests were performed on bolted and welded connections. The tests were designed and instrumented to provide validation data for the development of detailed numerical models that will predict the response of specimens up to total rupture with good accuracy. The test specimens consisted of two plates that were connected through a number of bolts or welds and were loaded in direct shear. A special loading frame was used to dynamically load those specimens using a 2,250 lb pendulum that impacted the loading frame with different velocities. Similar specimens were also loaded under quasi-static conditions. The test data provided a basis for the development of high-fidelity numerical models that were

able to replicate the physical testing and predict the response of the specimens with high accuracy. Through the validation process, a number of crucial modeling aspects were identified as discussed.

## REFERENCES

- [1] M. Hadjioannou, D. Stevens, and M. Barsotti, "Development and Validation of Bolted Connection Modeling in LS-DYNA for Large Vehicle Models," presented at the 14th International LS-DYNA Users Conference, Detroit, MI, 2016.
- [2] M. Hadjioannou and D. Stevens, "Mitigation of Blast Injuries Through Modeling and Simulation: Task 2 Report: Simplified Modeling Approaches for Bolted Connections," United States Marine Corps via Protection Engineering Consultants, Quantico, VA, Sep. 2015.
- [3] G. R. Johnson and W. H. Cook, "Fracture characteristics of three metals subjected to various strains, strain rates, temperatures and pressures," *Eng. Fract. Mech.*, vol. 21, no. 1, pp. 31–48, Jan. 1985.
- [4] W. R. Whittington *et al.*, "Capturing the effect of temperature, strain rate, and stress state on the plasticity and fracture of rolled homogeneous armor (RHA) steel," *Mater. Sci. Eng. A*, vol. 594, pp. 82–88, Jan. 2014.
- [5] J. Effelsberg, A. Haufe, M. Feucht, F. Neukamm, and P. Du Bois, "On parameter identification for the GISSMO damage model," presented at the 12th International LS-DYNA Users Conferences, Detroit, MI, 2012.
- [6] *LS-DYNA Keyword Users Manual - Vol. I*. Livermore, CA: Livermore Software Technology Corporation (LSTC), 2017.
- [7] "Contact parameters - LS-DYNA Support." [Online]. Available: <http://www.dynasupport.com/tutorial/contact-modeling-in-ls-dyna/contact-parameters>. [Accessed: 05-May-2017].